

Olivocochlear Neuron Central Anatomy Is Normal in $\alpha 9$ Knockout Mice

M. CHRISTIAN BROWN^{1,2,3} AND DOUGLAS E. VETTER⁴

¹*Department of Otolaryngology, Harvard Medical School, Boston, MA, USA*

²*Harvard-MIT Division of Health Sciences and Technology, Cambridge, MA, USA*

³*Eaton-Peabody Laboratory, Massachusetts Eye and Ear Infirmary, 243 Charles St., Boston, MA 02114, USA*

⁴*Department of Neuroscience, Tufts University School of Medicine, Boston, MA 02111, USA*

Received: 19 May 2008; Accepted: 25 September 2008; Online publication: 22 October 2008

ABSTRACT

Olivocochlear (OC) neurons were studied in a transgenic mouse with deletion of the $\alpha 9$ nicotinic acetylcholine receptor subunit. In this $\alpha 9$ knockout mouse, the peripheral effects of OC stimulation are lacking and the peripheral terminals of OC neurons under outer hair cells have abnormal morphology. To account for this mouse's apparently normal hearing, it has been proposed to have central compensation via collateral branches to the cochlear nucleus. We tested this idea by staining OC neurons for acetylcholinesterase and examining their morphology in knockout mice, wild-type mice of the same background strain, and CBA/CaJ mice. Knockout mice had normal OC systems in terms of numbers of OC neurons, dendritic patterns, and numbers of branches to the cochlear nucleus. The branch terminations were mainly to edge regions and to a lesser extent the core of the cochlear nucleus, and were similar among the strains in terms of the distribution and staining density. These data demonstrate that there are no obvious changes in the central morphology of the OC neurons in $\alpha 9$ knockout mice and make less attractive the idea that there is central compensation for deletion of the peripheral receptor in these mice.

Keywords: superior olive, cochlear nucleus, acetylcholinesterase, auditory reflex, noise masking, cholinergic receptor

INTRODUCTION

Olivocochlear (OC) neurons form a descending pathway that begins in the superior olivary complex of the brainstem and ends in the cochlea. One group of OC neurons, medial (M) OC neurons, sends collateral branches to the cochlear nucleus en route to ending on outer hair cells (Fig. 1A). MOC neurons reduce the effects of masking noise and protect the cochlea from damage due to acoustic overstimulation (reviewed by Guinan 1996) by altering the active mechanical properties of the outer hair cells in the cochlea (Housley and Ashmore 1991; Dallos et al. 1997). Their effects are mediated via the release of acetylcholine, which activates a nicotinic receptor formed of $\alpha 9$ and $\alpha 10$ nicotinic receptor subunits (Elgoyhen et al. 1994, 2001; Sgard et al. 2002).

The creation of a transgenic mouse with a deletion of the $\alpha 9$ nicotinic acetylcholine receptor (nAChR) represents an opportunity to test what role the OC neurons play in hearing. $\alpha 9$ knockout mice have cochleas that are functionally de-efferented, evidenced in the fact that they show none of the traditional electrophysiological effects following OC bundle stimulation (Vetter et al. 1999; Maison et al. 2007). The peripheral terminals of MOC neurons in the knockout have abnormal morphology (Vetter et al. 1999). They consist of larger-than-normal terminals in a ratio of one or two per hair

Correspondence to: M. Christian Brown · Eaton-Peabody Laboratory · Massachusetts Eye and Ear Infirmary · 243 Charles St., Boston, MA 02114, USA. Telephone: +1-617-5733875; fax: +1-617-7204408; email: Chris_Brown@meci.harvard.edu

cell (Fig. 1B, top), whereas in wild types they are smaller terminals in a ratio of 1–5 (average, 3) per hair cell (Fig. 1B, bottom). The knockout mice have been tested behaviorally to determine whether basic measures of hearing have been influenced (May et al. 2002). In both quiet and continuous noise, thresholds for tone detection and measures of intensity discrimination were unchanged relative to control subjects and to mice of the CBA/CaJ strain. This is a surprising result, given that surgical lesions of the OC bundle in normal animals result in behavioral deficits for signal detection in noise (Dewson 1968; Trahoitis and Elliott 1970; May and McQuone 1995; Heinz et al. 1998).

One possible explanation for the knockout/lesion difference is that unlike surgically lesioned animals, knockout animals have developed without a functioning $\alpha 9$ nAChR, allowing for the possibility of compensatory involvement of other systems. One idea proposed (May et al. 2002) is that axon collateral branches given off to the cochlear nucleus by MOC neurons (Fig. 1A) compensate for loss of MOC action peripherally so that behavioral measures are unchanged. These branches act via a receptor that has yet to be identified but is different from that of the periphery, since $\alpha 9$ nAChR is not present in the brain (Elgoyhen et al. 1994).

If such central plasticity is present, the MOC neurons may have accompanying anatomical changes such as those seen in other areas of the central auditory pathway (DeBello et al. 2001). The present study investigates MOC central plasticity by characterizing the anatomical phenotype of the $\alpha 9$ knockout mouse. Our detailed examination of the central anatomy investigated whether there were any differences between knockout and wild-type strains in the

number of OC neurons and their dendritic patterns. Dendrites were examined because MOC neurons receive predominant synaptic input onto their dendrites (Helfert et al. 1988; Benson and Brown 2006). We devoted particular attention to the OC central branches to the cochlear nucleus, in light of the hypothesis of their involvement in compensation (May et al. 2002). Interestingly, our results demonstrate normal MOC central anatomy in knockout mice and make less attractive the hypothesis of changes in OC central properties as a compensatory mechanism. The results are of further interest because the normal central branches, sent to neurons expressing a non- $\alpha 9$ receptor subunit, are from the same MOC neurons that have abnormal peripheral branches (Vetter et al. 1999), sent to OHCs lacking a functional $\alpha 9$ subunit. The results, then, illustrate that the postsynaptic target plays a large role in defining terminal morphology.

METHODS

Animals

All experimental procedures on animals were in accordance with the National Institutes of Health guidelines for the care and use of laboratory animals and were performed under approved protocols at the Massachusetts Eye & Ear Infirmary and Tufts University School of Medicine. Mice with deletions of the $\alpha 9$ nAChR (knockouts) were created as described by Vetter et al. (1999). Central anatomical results are presented for these knockouts ($\alpha 9^{-/-}$, $n=7$ mice), wild-type littermates ($\alpha 9^{+/+}$, $n=7$ mice), and wild-type controls of the same strain (WT, $n=2$ mice);

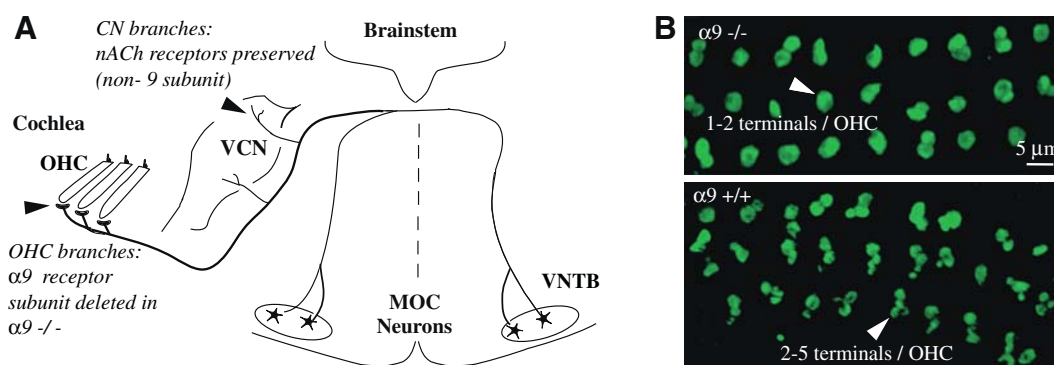


FIG. 1. **A** Schematic showing the medial olivocochlear (MOC) neurons in the brainstem, their collateral branches to the ventral cochlear nucleus (VCN), and their terminal projections to the outer hair cells (OHC) in the cochlea. Only projections to the left side are shown. In the knockout mouse strain investigated ($\alpha 9^{-/-}$), the $\alpha 9$ receptor subunit in the cochlea was deleted, but the receptor in the brainstem was preserved (it is believed to be a non- $\alpha 9$ cholinergic receptor). Most MOC neurons are located in the ventral nucleus of the trapezoid body (VNTB). **B** Surface view of MOC endings on outer

hair cells in a knockout ($\alpha 9^{-/-}$, top) and a wild-type littermate ($\alpha 9^{+/+}$, bottom). Endings were immunostained for synaptophysin. Arrows point to enlarged endings in the $\alpha 9^{-/-}$ that are usually present in a ratio of one or two per hair cell, and to smaller, more numerous endings in the $\alpha 9^{+/+}$ that are similar to those in other wild-type strains (Vetter et al. 1999). This material is from the middle turns of the cochleas of two of the animals used for central analysis of MOC neurons.

peripheral anatomical results (Fig. 1B) are presented for a single knockout and a single wild-type littermate. The WT group was included (and compared to the $\alpha 9$ $+/+$ group) because it is in some sense a control for genetic drift of the $\alpha 9$ colony. The strain for all of these mice was 129 Sv/Ev. Results are also presented for mice of strain CBA/CaJ ($n=4$ mice); these mice were obtained from Jackson Laboratories. All mice were between 3 and 5 months old.

Histology

Stains for acetylcholinesterase (AChE) were performed as described previously (Brown and Levine 2008). Mice were anesthetized with ketamine (100 mg/kg, i.p.) and xylazine (20 mg/kg, i.p.) and sacrificed by intracardiac perfusion with physiological saline followed by 4% paraformaldehyde in 0.1 M sodium phosphate buffer pH 7.2. After post-fixing for approximately 1 h, brainstems were dissected and immersed in the same fixative for an additional 1 h, then immersed in 30% sucrose overnight. Sections were cut (80 μ m thickness) in the transverse plane on a freezing microtome. Sections were stained for AChE by the Koelle indirect method (Koelle and Friedenwald 1949), modified according to Osen et al. (1984), by the following protocol: First, sections were incubated for 30 min in acetylthiocholine medium, rinsed in distilled water, incubated for 1 min in 4% sodium sulfide solution (pH 7.8), rinsed, incubated for 30 s in 1% silver nitrate, and rinsed again. The sections were mounted on slides, dried, counterstained with neutral red and then dehydrated, and coverslipped.

Cochleas were decalcified by overnight immersion in PBS-buffered 8% EDTA, then stripped of bone and the organ of Corti was dissected out. Immunostaining of synaptic endings on outer hair cells used a monoclonal antibody to synaptophysin (Chemicon; final dilution 1:1,000) with overnight incubation at 4°C. Secondary antibody was an anti-mouse Oregon Green antibody (Molecular Probes/Invitrogen) used at 1:500. Standard confocal microscopy was performed on a Leica TCS SP2 AOBS equipped confocal microscope.

Analysis

Counts of somata and of collateral branches to the cochlear nucleus were made using a compound microscope with $\times 10$ and $\times 60$ lenses. Only somata entirely within the section were counted. All somata were counted; there was no correction applied to the counts. Individual MOC dendrites were drawn with the $\times 10$ and $\times 60$ lenses. The length and orientation of an individual dendrite was then approximated by a vector beginning at the soma and ending at the tip.

Length of this vector was used as dendrite length and angle (from dorsal, 0°) was used for dendrite angle (Fig. 4). Intertwined dendrites were difficult to tease apart so we were only able to study dendrites that were relatively isolated from other stained elements. Only individual dendrites were considered; all the dendrites from individual neurons could not be reconstructed.

Quantitative measures of the innervation area (Fig. 10) were made by acquiring images with a $\times 10$ lens and a Hamamatsu CCD digital camera. Using Metamorph Image (Universal Imaging Corp.) and a computer-aided anatomy system, the images were thresholded (Fig. 7B) and compared to the micrographs before thresholding (Fig. 7A). The threshold level was set low enough so that all AChE-stained branches were included but not so low that artifact and non-stained structures (e.g., darkly counterstained neurons) were included. The edges of this optimal threshold were sharp and well defined. Only the cochlear nucleus was considered so stained axons in the OC bundle were not part of this analysis. The area of the stained regions in the thresholded sections (i.e., black regions in Fig. 7B) was measured using Image J. Statistical tests were considered significant for $p < 0.05$.

RESULTS

OC somata

OC neurons and their collateral branches were visualized using stains for acetylcholinesterase (Schuknecht and Nomura 1965; Osen 1969; Brown and Howlett 1972; Warr 1975; Martin 1981; White and Warr 1983; Osen et al. 1984; Brown and Levine 2008). Available data suggest that this stain is a specific marker for OC neurons in the mouse superior olivary complex because it yields essentially the same spatial distribution and number as retrograde labeling of OC neurons (Brown and Levine 2008). On this basis, we will presume that AChE staining is a marker for OC neurons in the superior olivary complex. MOC somata and their dendrites were darkly stained for AChE in all strains tested including $\alpha 9$ knockouts (Fig. 2A) and wild types (Fig. 2B). MOC neurons have large somata and were located in the ventral nucleus of the trapezoid body (VNTB), as described previously by retrograde labeling studies in other strains of mice (Campbell and Henson 1988; Brown and Levine 2008) and rat (Vetter et al. 1991; Vetter and Mugnaini 1992). Their distribution in all strains extends a considerable distance in the rostral-caudal direction, beginning somewhat caudal to the lateral superior olivary nucleus (LSO) and extending rostrally to the caudal part of the ventral nucleus of the lateral

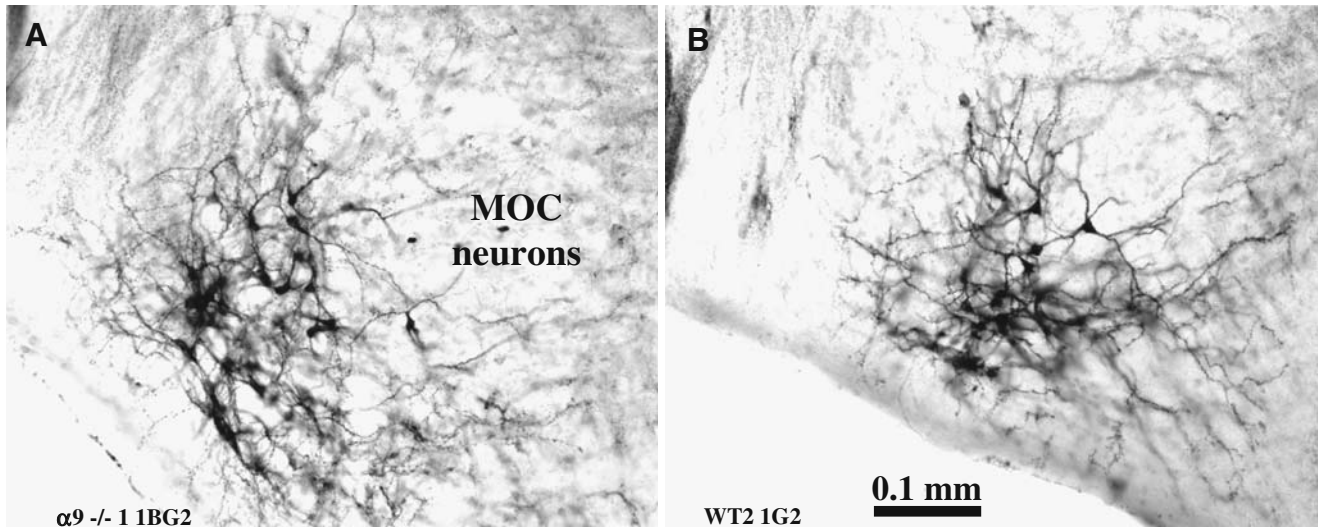


FIG. 2. Micrographs showing the similar appearance of AChE-stained MOC somata in a knockout ($\alpha 9^{-/-}$, **A**) and wild type (*WT*, **B**) of the same strain. In both panels, long dendrites are visible extending especially in the medial direction (*toward the right*). Somata are located in the VNTB rostral to the lateral superior olive on the left side of the brainstem.

lemniscus. In the present study, the average number of MOC neurons in the VNTB of one side of the brain ranged between strains from 172.6 to 195.0. These averages were not different between the strains (Fig. 3A, see legend). A few large OC neurons were

located just dorso-medial to the LSO in a region identified as the dorsal periolivary nucleus (DPO). Although it is not clear that these DPO neurons are MOC neurons, they bear similarities to MOC neurons in the VNTB except that their dendrites are more

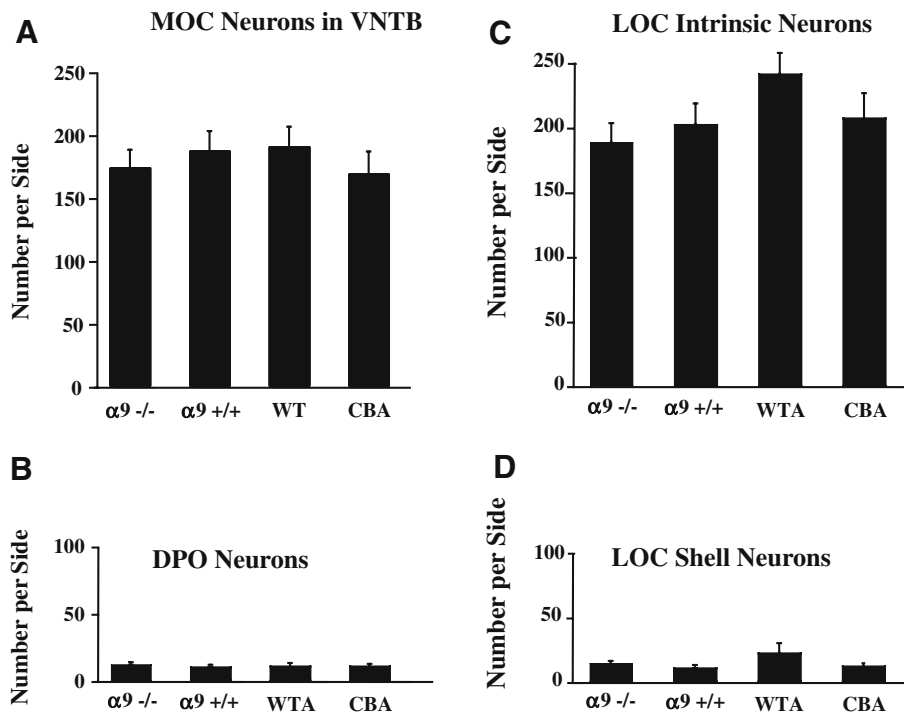


FIG. 3. Counts of **A** MOC neurons in VNTB, **B** DPO neurons, **C** LOC intrinsic neurons, and **D** LOC shell neurons. Data are from knockout mice with deletions of the $\alpha 9$ receptor ($\alpha 9^{-/-}$, $n=13$ superior olives), wild-type littermates ($\alpha 9^{+/+}$, $n=11$ superior olives), wild-type controls of the same strain (*WT*, $n=4$ superior olives), and

CBA controls ($n=7$ superior olives). Bars show the mean values and error bars show one SEM. For each panel, no statistically significant differences (ANOVA tests) were observed between the four groups, or between three groups formed by combining the $+/+$ and *WT* into a single group.

symmetric about the soma (Brown and Levine 2008). The number of DPO neurons was small and again did not differ between strains (on one side of the brain the average number of DPO neurons ranged from 10.7 to 12.8, Fig. 3B).

A second group of OC neurons, lateral (L) OC neurons, has smaller somata that are distributed within and on the borders of the LSO. LOC somata were also stained for AChE, but less darkly than MOC neurons, as reported in previous studies (White and Warr 1983). Sometimes the initial portions of the LOC primary dendrites were stained, but LOC axons were unstained. AChE-stained LOC neurons were divided into intrinsic neurons, whose somata were within the LSO, and shell neurons, whose somata were on the margins of the LSO (Vetter and Mugnaini 1992). Counts of LOC somata (Fig. 3C, D) showed no significant differences between strains (see Fig. 3 legend). We compared intrinsic neuron counts subdivided according to position in either the medial lobe or the lateral lobe of the LSO; they were also similar between strains (data not shown).

Other structures that were stained less darkly than OC neurons were the facial motor nucleus just caudal to the superior olivary complex and the trigeminal motor nucleus just rostral and dorsal to the complex. This staining difference was not caused by any difference in processing from section to section because it could be appreciated even when OC neurons and a portion of the facial motor nucleus appeared within the same section. The reaction

product in these motor nuclei was brown in color and occupied the extracellular space in the general vicinity of the neurons rather than the black reaction color that occurred within the OC neurons. The reason for this difference in staining is not clear.

MOC dendrites

MOC neurons in knockout and wild-type strains have extensive dendrites (Fig. 2). We studied the dendrites by plotting their lengths in polar format as a function of their orientation (Fig. 4) in order to determine whether they show the elongations in the medial direction as reported in CBA mice (Brown and Levine 2008). Dendrite lengths were approximated by a straight line segment from origin at the somata to their tip and their orientations by the angle of this segment with respect to the dorsal direction. Included in Figure 4 are dendrites from MOC neurons in the VNTB (filled symbols) and dendrites from neurons in DPO (open symbols). For VNTB neurons, the average length of the $\alpha 9^{-/-}$ dendrites was $148.4 \mu\text{m}$ (SEM $5.4 \mu\text{m}$, $n=181$) and for the $\alpha 9^{+/+}$ mice was $160.6 \mu\text{m}$ (SEM $4.7 \mu\text{m}$, $n=169$) and there was no significant difference between the two averages (t value -1.69 , $p=0.09$). These values are similar to that for CBA mice (avg. length $150.4 \mu\text{m}$, SEM $5.7 \mu\text{m}$, $n=136$ as reported previously by Brown and Levine 2008). For DPO neurons, the average lengths of the dendrites were also similar for the two strains ($\alpha 9^{-/-}$ dendrites averaged $147.1 \mu\text{m}$ (SEM $10.0 \mu\text{m}$, $n=17$); $\alpha 9^{+/+}$

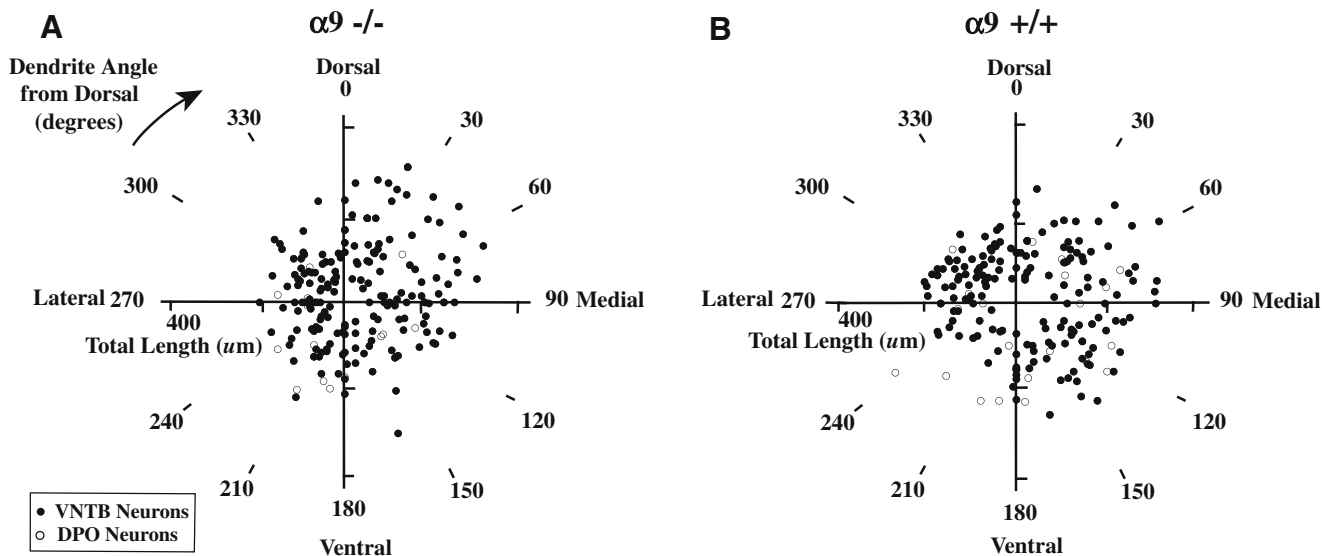


FIG. 4. Dendrite lengths plotted as a function of dendrite angle (in degrees from dorsal) for: **A** knockout mice with deletions of the $\alpha 9$ receptor ($\alpha 9^{-/-}$), 181 dendrites from three mice; and **B** wild-type littermates ($\alpha 9^{+/+}$), 169 dendrites from three mice. Data are mostly from MOC neurons located in VNTB (filled symbols) and a few

neurons in DPO (open symbols). The Rayleigh test for randomness of a circular distribution (Batschelet 1981) was significant for both samples, indicating that they are skewed, non-random distributions (**A**, $r=0.13$, $Z_{\text{observed}}=3.15$, $Z_{\text{critical}}=1.64$ for $\alpha=0.05$; **B**, $r=0.14$, $Z_{\text{observed}}=23.05$, $Z_{\text{critical}}=1.64$ for $\alpha=0.05$).

dendrites averaged $180.1 \mu\text{m}$ (SEM $12.4 \mu\text{m}$, $n=23$, not significantly different, t value -1.96 , $p=0.06$).

Dendrites of VNTB neurons in both strains of mice were often more numerous and longer in the medial direction than in the lateral direction, which can be appreciated from an examination of individual dendrites (Fig. 2). We determined, using the Rayleigh test for a uniformly circular distribution (see Fig. 4 legend), that the distributions of dendrites were non-uniform. Our samples contained more dendrites pointing medially than laterally. For example, in $\alpha 9^{-/-}$ mice there were 96 dendrites oriented toward the medial direction (angles $0-179^\circ$ in Fig. 4) whereas and only 85 dendrites toward the lateral direction. The medial dendrites were also longer (average length $178.5 \mu\text{m}$) compared to lateral dendrites (average length $114.4 \mu\text{m}$), a statistically significant difference (t value 6.523 , $p=0.0001$). For dendrites of VNTB neurons in $\alpha 9^{+/+}$ mice, the 104 dendrites toward the medial direction averaged $181.4 \mu\text{m}$ in length whereas those 88 dendrites toward the lateral direction averaged $141.1 \mu\text{m}$, also significantly different (t value 5.044 , $p=0.0001$). Dendrites of DPO neurons, however, had more similar lengths in the lateral vs. medial directions (Fig. 4). All of these trends have previously been reported for CBA mice (Brown and Levine 2008).

OC collateral branches to the cochlear nucleus

Stained axons were observed emanating from both VNTB and DPO neurons and they traveled dorsally to

form the OC bundle, which was well stained in all the strains of mice examined (Fig. 5). Collateral branches from axons were visible along the OC bundle's course on the entire medial edge of the cochlear nucleus (Fig. 5B). In this region, counts were made of individual branches just after they came off the OC bundle. There was no fading of the AChE stain in mid-section so all branches could be counted. The number of branches is plotted for the several strains examined in Figure 6A. The average number of branches to the cochlear nucleus on one side ranged between strains from 127.0 and 140.5, and when normalized by the numbers of MOC neurons ranged from 0.72 to 0.74. There was no significant difference between strains (see Fig. 6 legend). On entering the cochlear nucleus, the branches often ramified and became intermixed. No stained branches were observed entering the ventral cochlear nucleus from sources other than the OC bundle. MOC neurons also give off branches to the vestibular nuclei (Brown 1993). These collaterals were difficult to count because there was more background reaction product in this area of the brainstem and because these branches often began branching just after coming off the parent axons. However, there was qualitative similarity in the frequency of these branches to the vestibular nuclei in all strains examined.

Branch terminations

OC collateral branches terminate mainly in edge regions and to a lesser extent in the core of the

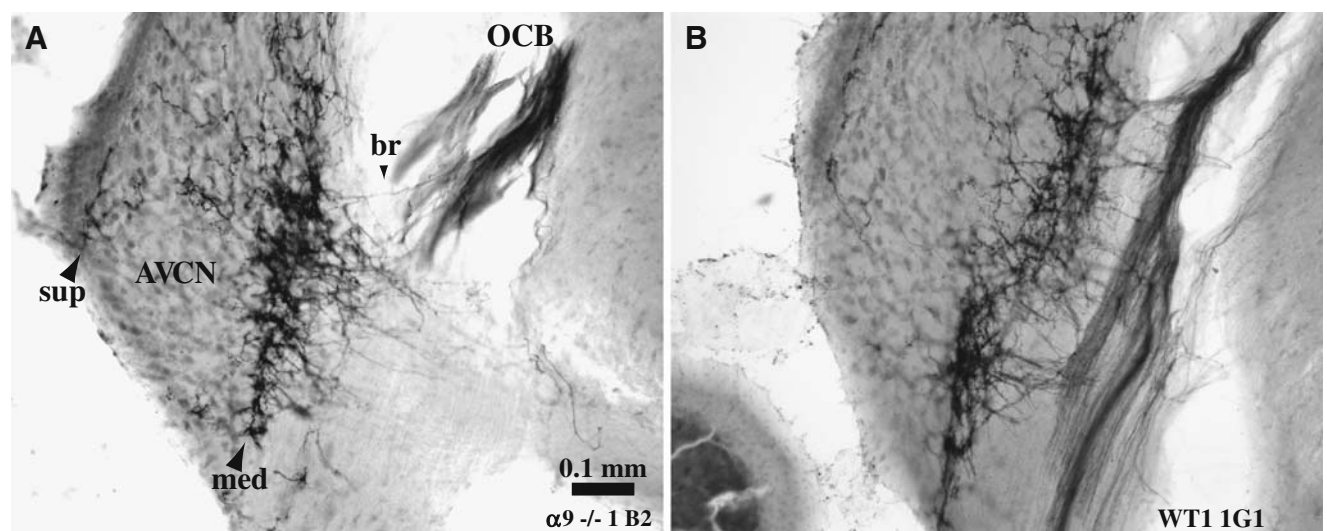


FIG. 5. Photomicrographs of the olivocochlear bundle (OCB) and its branches (*br*) stained black for AChE. Shown are sections from **A** a knockout lacking the $\alpha 9$ receptor ($\alpha 9^{-/-}$), and **B** a wild-type control (WT). In these sections, most of the branches form endings at the medial edge (*med*), some in the core of the anteroventral cochlear

nucleus (AVCN), and a few at its superficial edge (*sup*). To be consistent with the other figures of the paper, these images of the cochlear nucleus on the *right side* have been reversed to appear as cochlear nuclei on the *left side*.

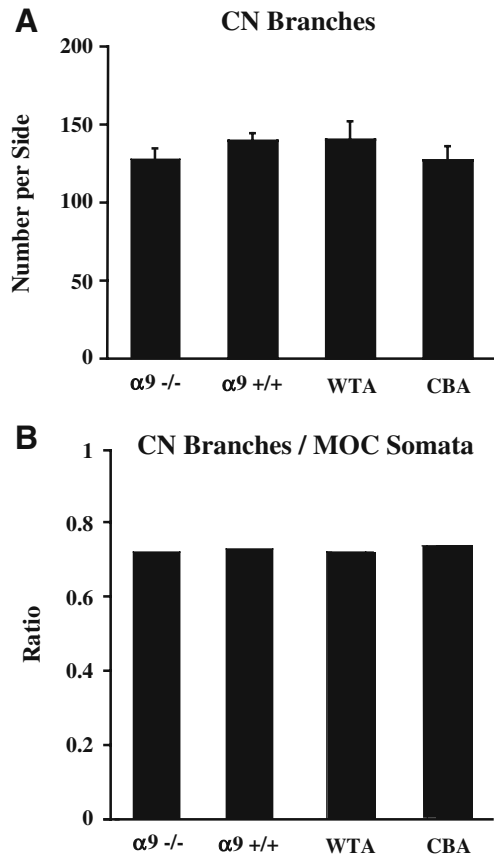


FIG. 6. **A** Counts of OC branches directed toward the cochlear nucleus in knockout mice with deletions of the $\alpha 9$ receptor ($\alpha 9^{-/-}$, avg. of 128.1 branches (SEM 5.7) in $n=13$ cochlear nuclei), wild-type littermates ($\alpha 9^{+/+}$, avg. of 139.4 branches (SEM 4.2) in $n=14$ cochlear nuclei), wild-type controls (WT, avg. of 140.5 branches (SEM 11.2) in $n=4$ cochlear nuclei) and CBA controls (avg. of 127 branches (SEM 8.6) in $n=7$ cochlear nuclei). Bars show the mean values and error bars show one SEM. No statistically significant differences were observed (ANOVA test) between the four groups, or between three groups formed by combining the $+/+$ and WT into a single group. **B** Average ratio of cochlear nucleus (CN) branches/MOC somata for each of the four groups.

ventral cochlear nucleus with almost no staining in the dorsal cochlear nucleus (Martin 1981; Osen et al. 1984; Brown et al. 1988; Brown 1993). Figure 7A shows staining of the terminations of branches in a section of the anteroventral cochlear nucleus (AVCN) just rostral to the entry of the auditory nerve. There is dense staining of branches at the medial edge, with some branches straying into the core of the cochlear nucleus especially ventrally where the nerve root is large. There is additional staining at the lateral and dorsal edges of the AVCN. Figure 7A is from a knockout mouse, but wild-type and CBA mice showed the same general pattern of branch terminations except that CBA mice may have less staining from branches that terminate at the lateral edge. Except for this difference, the darkness and appearance of staining in the cochlear nucleus was similar in all

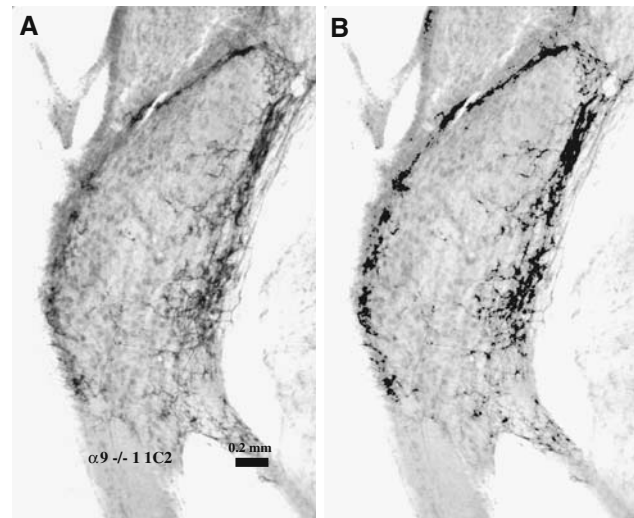


FIG. 7. Thresholding method applied to one section through the AVCN just rostral to the auditory nerve root. **A** Image of an AChE-stained section showing staining of branch terminations mainly at the margins of the nucleus in a knockout mouse. **B** The same section after thresholding.

strains of mice. Individual branches that terminated in edge regions were extensively intertwined, but individual branches in the core could sometimes be separated. Examples of core branches from AVCN are shown from a knockout and a CBA mouse in Figure 8. As in all branches, the initial portion of the branch is thin. Then, the branch increases in diameter and forms frequent swellings, which have been demonstrated to be sites where they form synapses (Benson

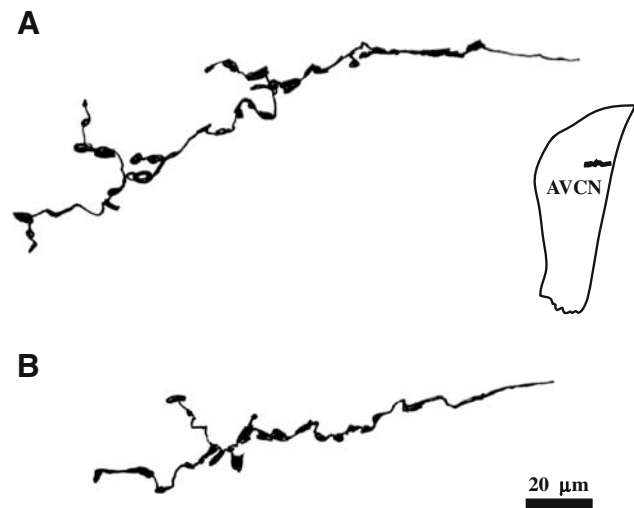


FIG. 8. Camera lucida drawings illustrating the similar appearance of AChE-stained branches from a knockout (**A**) and from a CBA mouse (**B**). Both branches were directed to a similar location in the core of AVCN (see inset). Here, they form numerous swellings and small sub-branches. The branches begin as thinner segments without swellings (right part of drawing) as they originate from axons in the olivocochlear bundle.

and Brown 1990). In terms of the number of swellings per length and the shapes of the swellings, the terminal morphology of the branches in the knockout did not obviously differ between strains.

For a quantitative analysis of the stained branches, we used “thresholding” to quantify the staining (Fig. 7B). These thresholded regions represent “filled in” regions of branch termination much as the eye fills in the stained region of cochlear nucleus when the sections are viewed with a low magnification ($\times 4$) objective. The stained area includes all parts of the collateral branches, but is likely dominated by the thicker parts with swellings (Fig. 8). Figure 9 is an atlas of thresholded cochlear nucleus sections from an $\alpha 9^{-/-}$ and a wild-type mouse. The two example atlases shown have small individual differences in staining, but these differences were not consistently observed between strains. In all strains, the most staining was at the medial border of the cochlear nucleus. There was also staining at the dorsal border of the ventral cochlear nucleus, just beneath the granule cell lamina. This granule cell lamina divides the ventral from the dorsal subdivisions of the nucleus. There is lesser edge staining at the superficial edge (lateral border of the nucleus). This staining did not extend as far rostrally as the medial edge staining. Some staining was present in the subpenduncular corner, a small region of granule cells just ventral to the inferior cerebellar peduncle (Mugnaini et al. 1980), and a very small amount of staining extended dorsally along the medial border of the dorsal

cochlear nucleus. Staining was also present within the core of the ventral cochlear nucleus, especially in the caudal auditory nerve root where it occurred within islands of cells between the incoming fascicles of auditory nerve fibers. Another core staining area is found several sections rostral to the nerve root (e.g., Fig. 8). More isolated branches are seen elsewhere in the core with the exception of the most rostral part of AVCN and the caudal-most part of posteroventral subdivision of the cochlear nucleus (PVCN), which lacks staining. In particular, the octopus cell area in caudal PVCN contained minimal staining.

Quantitative comparisons of the stained areas of two $\alpha 9$ knockout and two wild-type mice are shown in Figure 10. There is little difference in the total staining between the four mice (panel A). This total staining follows a pattern in the rostro-caudal dimension (x -axis) where the amount of staining is small caudally, increases toward the middle of the cochlear nucleus, and then falls again at the rostral parts. A dip in this pattern is seen in the middle section containing the auditory nerve root, which is a cell-poor region of the nucleus. There was no significant difference in total staining between the animals (see Fig. 10 legend). We parcellated the subregions of staining into medial, dorsal, and lateral edges and also the core (Fig. 10, panels B–E). Core staining was defined as staining that was physically separated from edge staining, usually by branches oriented perpendicularly to the large patches of edge staining. A few such branches can be seen emanating from the large

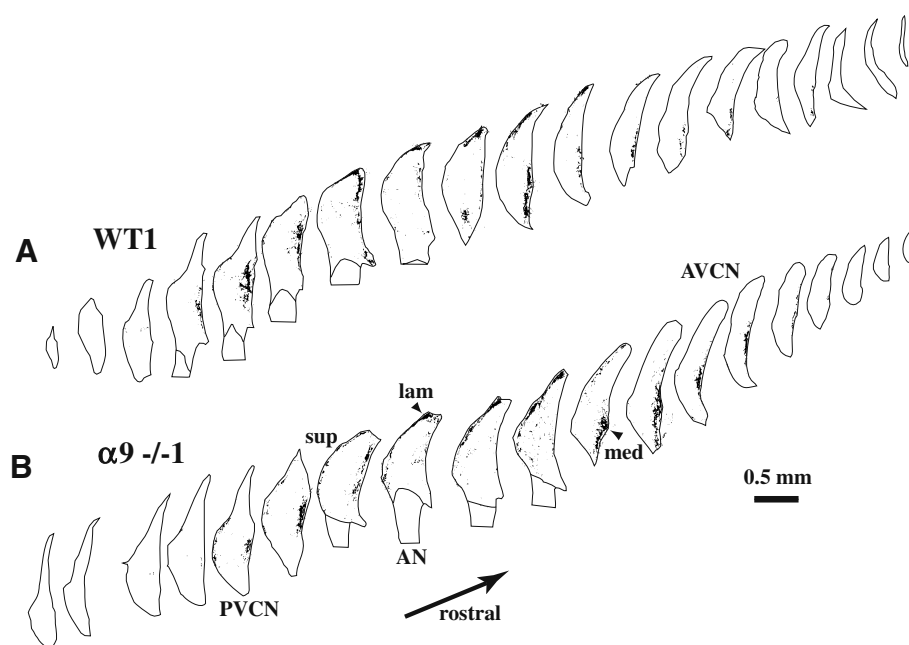


FIG. 9. Atlas sections showing the generally similar distribution of branch staining in the ventral cochlear nucleus of a wild-type control (A) and a knockout (B). There is a rich innervation of the edges of the nucleus (*med*: medial edge; *lam*: lamina of granule cells at the dorsal edge; *sup*: superficial layer at the lateral edge). Staining tapers off rostrally and caudally. The *black* represents AChE staining in images after thresholding (see Fig. 7).

FIG. 10. Area of stained branches in the cochlear nucleus as a function of rostro/caudal distance for two knockouts ($\alpha 9^{-/-}$, solid lines) and two wild types (WT, dashed lines). **A** Total area for the four individual animals. The remaining panels show averaged staining for two knockouts and two wild types in **B** medial edge, **C** dorsal edge, **D** lateral edge, and **E** core. Area was measured from images after thresholding (Figs. 7 and 9). The four cases were aligned using the “dip” in total staining (**A**) that occurs in the auditory nerve root. ANOVA tests revealed no section-by-section difference in the total staining, both between the four animals were compared as four groups and between two groups formed by the averages of the knockouts and the averages of the wild types.

patches of medial-edge staining in Figure 7. Of the subregions, the medial edge shows the greatest amount of staining and the other edge regions show lesser amounts. The core shows the least amount of staining. Medial staining extends more rostrally than the other subgroups. In the two animals used for this atlas, there were slightly higher amounts of staining at the lateral edge in the knockouts, but this was not observed in qualitative examination of other knockouts. There were no clear differences between knockout and wild type in the other subregions.

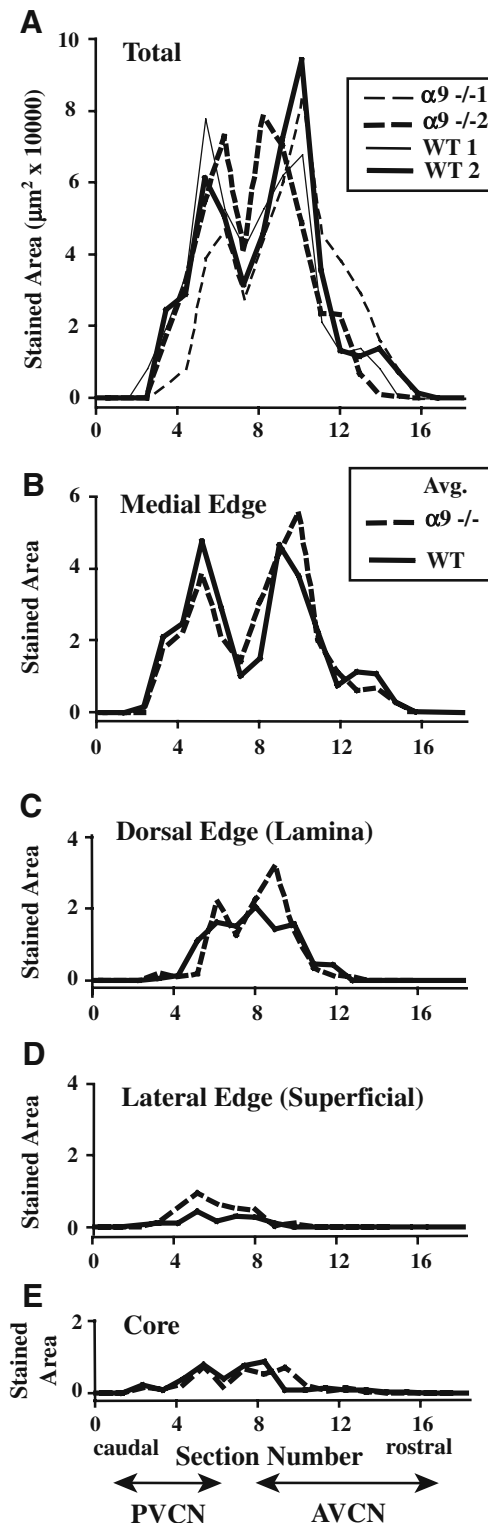
DISCUSSION

AChE stains for OC neurons

We relied on AChE stains to mark MOC somata within the superior olivary complex (Warr 1975; White and Warr 1983; Osen et al. 1984). The dark staining and low background make the AChE stain an excellent marker for counting small elements such as individual cochlear nucleus branches as we have done in the present study. Available data also support the idea that the AChE stain is a specific marker for OC branches to the cochlear nucleus since the branches emanate from stained axons in the OC bundle and since their morphology and terminations are similar to those labeled by tracers (Brown et al. 1991). Most OC branches are probably from MOC neurons in VNTB. It is not clear whether DPO neurons form central collaterals. No non-olivocochlear source of stained branches to the ventral cochlear nucleus was observed in our material.

OC somata and dendrites

Our study is the first to demonstrate normal numbers of OC somata in the $\alpha 9$ knockout mouse. Previous work (Vetter et al. 1999) demonstrated normal position of the olivocochlear bundle without examination of other aspects of central morphology. The normal number of MOC somata indicates that deletion of the peripheral receptor and consequent block of the peripheral effects, which alter peripheral



terminal morphology (Vetter et al. 1999), does not affect this system’s number and distribution of somata in the brain.

MOC dendrites are extensive (Adams 1983; White and Warr 1983; Osen et al. 1984; Vetter and Mugnaini 1992; Warr et al. 2002; Sánchez-González et al. 2003).

In CBA mice (Brown and Levine 2008), the dendrites are elongated in the medial direction. Our results (Fig. 4) demonstrate that this elongation is also present in the knockout mouse and in wild types of the 129 Sv/Ev strain. This direction is the route by which the predominant input arrives from the cochlear nucleus and presumably much of this input is onto these dendrites. Previous results in CBA mice (Brown and Levine 2008) show that dendrites are also somewhat elongated in the rostral direction, perhaps to receive descending input from higher centers. Individual dendrites that were isolated from other dendrites were the only ones that could be reconstructed and could theoretically have biased us to consider only a subclass of dendrites. The effect of this sampling is difficult to estimate.

OC collateral branches to the cochlear nucleus

Our data suggest that independent of mouse strain, there are about 130 OC collateral branches to each cochlear nucleus. The stability of the ratio between the strains investigated here suggests stability in the central collateral branch system in the cochlear nucleus in the $\alpha 9$ knockout mouse. The number of OC branches to the cochlear nucleus has not been reported previously. In a limited sample of HRP-labeled MOC axons, our previous studies demonstrated that the percent of axons that branch was about 2/3 for OC axons directed to the cochlear basal half (Brown et al. 1988; Brown 1993), the area where many MOC neurons terminate. In the present study, we computed the ratio of branches to cell bodies as between 0.70 and 0.74 (Fig. 6B), a similar number to the percent of axons that branch. This comparison assumes that each MOC neuron gives off a single axon and that each axon that branches forms only one branch to the cochlear nucleus. Our rationale for using the number of MOC neurons, rather than LOC neurons, for computing the ratio (Fig. 6B) was based on our earlier work (Brown et al. 1988) showing that only the thick, MOC axons form cochlear nucleus branches. The work of others (Ryan et al. 1990; Horvath et al. 2000) apparently demonstrates branches from LOC neurons but since they are distributed mainly to the core and since LOC axons were not well stained for AChE, they were apparently not visualized in the present study.

Our results have produced the first atlas of the branch terminations in the cochlear nucleus (Fig. 9) and represent the first quantification of the staining (Fig. 10). The regions targeted by the branches were similar to those described previously (Martin 1981; Osen et al. 1984; Brown et al. 1988; Brown 1993). There was a dense innervation of the medial edge of the ventral cochlear nucleus as well as the dorsal edge

(granule cell lamina dividing the ventral from the dorsal subdivisions of the cochlear nucleus). These regions showed the largest stained areas (Fig. 10B, C). Lesser amounts of stained area were present at the lateral edge of the nucleus. The core of the ventral cochlear nucleus received the smallest amount of stained area; in our results, this occurs sporadically throughout the middle of the cochlear nucleus. In previous results of Martin (1981), core staining was found mainly in the PVCN and the reason for this difference is not clear. One possibility is that the previous results are from mice of the C57 strain, which has an age-related hearing loss (Li and Borg 1991). The age of the mice used in the present study was 3–5 months, within the age range for normal hearing (May et al. 2002).

The functional role of the OC branches to the cochlear nucleus is still being worked out. The endings of these branches contain round synaptic vesicles and form asymmetric synapses (Benson and Brown 1990), suggesting that they have an excitatory effect. During OC feedback to the periphery, the branches may compensate for reduced sensitivity of the cochlea by increasing the responses of certain neurons in the cochlear nucleus (Benson and Brown 1990). This type of compensation could theoretically be important in neurons that code for the absolute intensity of a sound. In support of this theory, electrophysiological recordings (Mulders et al. 2003) demonstrate that specific neurons (those with onset chopper responses to sound) are excited by stimulation of the OC bundle in a fundamentally different way from other neurons of the cochlear nucleus. Similar indications of an excitatory effect of the branches are suggested from work in slice preparations in which T stellate (multipolar) neurons can be excited by cholinergic input (Fujino and Oertel 2001).

Since neither the $\alpha 9$ nor $\alpha 10$ nicotinic receptor subunit is present in the cochlear nucleus, the subunit composition making up the cholinergic receptor for OC central branches likely contains nAChR subunits more typical of the brain. Several studies suggest that this central receptor is the $\alpha 7$ receptor. Anatomically, the edge regions of the cochlear nucleus (where OC branches terminate) show binding to α -bungarotoxin (Morley et al. 1977; Hunt and Schmidt 1978), which tightly binds the $\alpha 7$, $\alpha 8$, $\alpha 9$, and $\alpha 10$ subunits. Because $\alpha 9$ and $\alpha 10$ subunits are not found in the brain, and $\alpha 8$ has thus far been localized only to chick retina, the most likely candidate expressed by these neurons that binds bungarotoxin is the $\alpha 7$ subunit. These same regions show immunostaining (Yao and Godfrey 1999) and the presence of mRNA for this receptor (Happe and Morely 1998). The pharmacological profile of the effect of ACh on cochlear

nucleus stellate cells is also consistent with the involvement of an $\alpha 7$ receptor as well as the presence of other cholinergic receptors (Fujino and Oertel 2001).

Relevance for plasticity in the knockout

The present study indicates that the central neuroanatomy of OC neurons is normal in mice with deletions of the $\alpha 9$ nAChR. The $\alpha 9$ knockout has a normal complement of MOC and LOC somata as well as a normal complement of collateral branches to the cochlear nucleus. The normal central anatomy is interesting because the peripheral terminals of MOC neurons in this mouse strain have clearly abnormal morphology (Vetter et al. 1999; Fig. 1B). Apparently, the deletion of the receptor at the peripheral synapse affects the peripheral morphology whereas the persistence of the receptor at the central synapse preserves the central morphology. Our results highlight the role played by postsynaptic targets in directing synaptogenic programs and show for the first time that a receptor knockout can underlie the very specific (rather than global) morphological changes in a presynaptic neuron.

Anatomical changes are the underlying manifestation of plasticity in function in some cases (DeBello et al. 2001). If the central branches of OC neurons underlie plastic changes in hearing in the knockout, we might have expected changes in their number or morphology, but these were not observed. Our data on the cochlear nucleus branches in knockouts do not exclude the possibility of altered morphology in some aspect of the anatomy that is beyond the resolution of the present study's methods, such as a change in the ultrastructure of the synapse or a changed physiology without accompanying anatomical changes. But our results do exclude large anatomical changes that have been observed in other systems that apparently result in plasticity of neural function.

Our findings demonstrate the stability of the central anatomy of the OC system in $\alpha 9$ knockout mice. Thus, they make less attractive the hypothesis that central plasticity, such as changes in the collateral branches to the cochlear nucleus, accounts for the normal measures of hearing in these animals (May et al. 2002). It remains possible that auditory cues used for signal detection involve centers or neurons of the cochlear nucleus not innervated by the MOC collaterals, or that the collaterals merely fine tune such detection, thus rendering changes below the level of resolution of behavioral tests. Given the highly parallel and divergent nature of auditory processing, even at lower brainstem nuclei, this could involve numerous other auditory nuclei besides, or working in conjunction with, the cochlear nucleus.

ACKNOWLEDGMENTS

Supported by NIH grants DCD 01089 (to MCB), DCD 006258 (to DEV), P30 DC005209 (to MEEI), and P30 NS047243 (to Tufts CNR). Preliminary results of this study were presented in abstract form at the Association for Research in Otolaryngology Midwinter Meeting, February, 2006.

REFERENCES

- ADAMS JC. Cytology of periolivary cells and the organization of their projections in the cat. *J. Comp. Neurol.* 215:275–289, 1983.
- BATSCHLET E. *Circular Statistics in Biology*. London, Academic, 1981.
- BENSON TE, BROWN MC. Synapses formed by olivocochlear axon branches in the mouse cochlear nucleus. *J. Comp. Neurol.* 295:52–70, 1990.
- BENSON TE, BROWN MC. Ultrastructure of synaptic input to medial olivocochlear neurons. *J. Comp. Neurol.* 499:244–257, 2006.
- BROWN MC. Fiber pathways and branching patterns of biocytin-labeled olivocochlear neurons in the mouse brainstem. *J. Comp. Neurol.* 337:600–613, 1993.
- BROWN JC, HOWLETT B. The olivo-cochlear tract in the rat and its bearing on the homologies of some constituent cell groups of the mammalian superior olivary complex: a thiocholine study. *Acta. Anat.* 83:505–526, 1972.
- BROWN MC, LEVINE JL. Dendrites of medial olivocochlear (MOC) neurons in mouse. *Neurosci.* 154:147–159, 2008.
- BROWN MC, PIERCE S, BERGLUND AM. Cochlear-nucleus branches of thick (medial) olivocochlear fibers in the mouse: a cochleotopic projection. *J. Comp. Neurol.* 303:300–315, 1991.
- BROWN MC, LIBERMAN MC, BENSON TE, RYUGO DK. Brainstem branches from olivocochlear axons in cats and rodents. *J. Comp. Neurol.* 278:591–603, 1988.
- CAMPBELL JP, HENSON MM. Olivocochlear neurons in the brainstem of the mouse. *Hear. Res.* 35:271–274, 1988.
- DALLOS P, HE DZZ, LIN X, SZIKLAI I, MEHTA S, EVANS BN. Acetylcholine, outer hair cell motility, and the cochlear amplifier. *J. Neurosci.* 17:2212–2226, 1997.
- DEBELLO WM, FELDMAN DE, KNUDSEN EI. Adaptive axonal remodeling in the midbrain auditory space map. *J. Neurosci.* 21:3161–3174, 2001.
- DEWSON JH. Efferent olivocochlear bundle: some relationships to stimulus discrimination in noise. *J. Neurophysiol.* 31:122–130, 1968.
- ELGOYHEN AB, JOHNSON DS, BOULTER J, VETTER DE, HEINEMANN S. Alpha 9: an acetylcholine receptor with novel pharmacological properties expressed in rat cochlear hair cells. *Cell* 79:705–715, 1994.
- ELGOYHEN AB, JOHNSON JB, BOULTER J, VETTER D, HEINEMANN S. Alpha 10: a determinant of nicotinic cholinergic receptor function in mammalian vestibular and cochlear mechanosensory cells. *PNAS* 98:3501–3506, 2001.
- FUJINO K, OERTEL D. Cholinergic modulation of stellate cells in the mammalian ventral cochlear nucleus. *J. Neurosci.* 21:7372–7383, 2001.
- GUINAN JJ, JR. *The physiology of olivocochlear efferents*. The Cochlea. P. Dallos, A. N. Popper and R. R. Fay. New York, Springer-Verlag: 435–502, 1996.
- HAPPE HK, MORELY BJ. Nicotinic acetylcholine receptors in rat cochlear nucleus: [125I]-alpha-bungarotoxin receptor autoradiography and in situ receptor autoradiography of alpha7 nAChR subunit mRNA. *J. Comp. Neurol.* 397:163–180, 1998.

- HELFFERT RH, SCHWARTZ IR, RYAN AF. Ultrastructural characterization of gerbil olivocochlear neurons based on differential uptake of 3H-D-Aspartic acid and a wheatgerm agglutinin-horseshoe peroxidase conjugate from the cochlea. *J. Neurosci.* 8:3111–3123, 1988.
- HEINZ RD, STILES P, MAY BJ. Effects of bilateral olivocochlear lesions on vowel formant discrimination in cats. *Hear. Res.* 116:10–20, 1998.
- HORVATH M, KRAUS KS, ILLING R-B. Olivocochlear neurons sending axon collaterals into the ventral cochlear nucleus of the rat. *J. Comp. Neurol.* 422:95–105, 2000.
- HOUSLEY GD, ASHMORE JF. Direct measurement of the action of acetylcholine on isolated outer hair cells of the guinea pig cochlea. *Proc. R. Soc. Lond. B.* 244:161–167, 1991.
- HUNT S, SCHMIDT J. Some observations of the binding patterns of alpha-bungarotoxin in the central nervous system of the rat. *Brain Res.* 157:213–232, 1978.
- KOELLE GB, FRIEDENWALD JS. A histochemical method for localizing cholinesterase activity. *Proc. Soc. Exp. Biol. Med.* 70:617–622, 1949.
- LI HS, BORG E. Age-related loss of sensitivity in two mouse genotypes. *Acta Otolaryngol.* 111:827–834, 1991.
- MAISON SF, VETTER DE, LIBERMAN MC. A novel effect of cochlear efferents: in vivo response enhancement does not require alpha9 cholinergic receptors. *J. Neurophysiol.* 97:3269–3278, 2007.
- MARTIN MR. Acetylcholinesterase-positive fibers and cell bodies in the cochlear nuclei of normal and reeler mutant mice. *J. Comp. Neurol.* 197:153–167, 1981.
- MAY BJ, McQUONE SJ. Effects of bilateral olivocochlear lesions on pure-tone intensity discrimination in cats. *Auditory Neurosci.* 1:385–400, 1995.
- MAY BJ, PROSEN CA, WEISS D, VETTER D. Behavioral investigation of some possible effects of central olivocochlear pathways in transgenic mice. *Hearing Res.* 171:142–157, 2002.
- MORLEY B, LORDEN JF, BROWN GB, KEMP GE, BRADLEY RJ. Regional distribution of nicotinic acetylcholine in rat brain. *Brain Res.* 134:161–166, 1977.
- MUGNAINI E, WARR WB, OSEN KK. Distribution and light microscopic features of granule cells in the cochlear nucleus of cat, rat, and mouse. *J. Comp. Neurol.* 191:581–606, 1980.
- MULDERS WHAM, PAOLINI AG, NEEDHAM K, ROBERTSON D. Olivocochlear collaterals evoke excitatory effects in onset neurones of the rat cochlear nucleus. *Hear. Res.* 176:113–121, 2003.
- OSEN KK. Cytoarchitecture of the cochlear nuclei in the cat. *J. Comp. Neurol.* 136:453–484, 1969.
- OSEN KK, MUGNAINI E, DAHL A-L, CHRISTIANSEN AH. Histochemical localization of acetylcholinesterase in the cochlear and superior olivary nuclei. A reappraisal with emphasis on the cochlear granule cell system. *Arch. Ital. Biol.* 122:169–212, 1984.
- RYAN AF, KEITHLEY EM, WANG Z-X, SCHWARTZ IR. Collaterals from lateral and medial olivocochlear efferent neurons innervate different regions of the cochlear nucleus and adjacent brainstem. *J. Comp. Neurol.* 300:572–582, 1990.
- SANCHEZ-GONZALEZ MA, WARR WB, LOPEZ DE. Anatomy of olivocochlear neurons in the hamster studied with FluoroGold. *Hearing Res.* 185:65–76, 2003.
- SCHUKNECHT HF, NOMURA Y. The efferent fibers in the cochlea. *Ann. Otol. Rhinol. Laryngol.* 74:289–303, 1965.
- SGARD F, CHARPENTIER E, BERTRAND S, WALKER N, CAPUT D, GRAHAM D, BERTRAND D, BESNARD F. A novel human nicotinic receptor subunit, alpha10, that confers functionality to the alpha-10 subunit. *Mol. Pharmacol.* 61:150–159, 2002.
- TRAHOITIS C, ELLIOTT DN. Behavioral investigation of some possible effects of sectioning the crossed olivocochlear bundle. *J. Acoust. Soc. Am.* 47:592–596, 1970.
- VETTER DE, MUGNAINI E. Distribution and dendritic features of three groups of rat olivocochlear neurons. A study with two retrograde cholera toxin tracers. *Anat. Embryol.* 185:1–16, 1992.
- VETTER DE, ADAMS JC, MUGNAINI E. Chemically distinct rat olivocochlear neurons. *Synapse* 7:21–43, 1991.
- VETTER DE, LIBERMAN MC, MANN J, BARHANIN J, BOULTER J, BROWN MC, SAFFIOTE-KOLMAN J, HEINEMANN SF, ELGOYHEN AB. Role of $\alpha 9$ nicotinic ACh receptor subunits in the development and function of cochlear efferent innervation. *Neuron* 23:93–103, 1999.
- WARR WB. Olivocochlear and vestibular efferent neurons of the feline brainstem: their location, morphology, and number determined by retrograde axonal transport and acetylcholinesterase histochemistry. *J. Comp. Neurol.* 161:159–182, 1975.
- WARR WB, BOCHE JEB, YE Y, KIM DO. Organization of olivocochlear neurons in the cat studied with the retrograde tracer cholera toxin-B. *J. Assoc. Res. Otolaryngol.* 3:457–478, 2002.
- WHITE JS, WARR WB. The dual origins of the olivocochlear bundle in the albino rat. *J. Comp. Neurol.* 219:203–214, 1983.
- YAO W, GODFREY DA. Immunolocalization of alpha4 and alpha7 subunits of nicotinic receptor in rat cochlear nucleus. *Hear. Res.* 128:97–102, 1999.